CREEP BEHAVIOR OF 1Cr0.5Mo STEEL . PART 2 – CHARACTERIZATION AND DATA PARAMETERIZATION IN THE EX-SERVICE CONDITION*

Levi de Oliveira Bueno[1]

Abstract

Constant stress testing was used for characterization of creep behavior of a 1Cr0.5Mo steel plate in the ex-service condition. The tests were performed on creep machines equipped with Andrade-Chalmers type profiles, high sensitivity SLVC transducer extensometry, high stability temperature controllers, and facilities for monitoring the creep curves with an automatic data logging system. Ten creep machines of this type were used in this research, in an experimental work that lasted for one year. Three temperature levels were selected: 538, 565 and 593°C, with stress in the range from 52 to 224 MPa producing rupture times varying from 5 to about 3950h. The creep curves were all followed with great scrutiny using data logger scanning rates which enabled storing thousands of readings in each case. The experimental analysis involved measurements of minimum creep rate, rupture time and final elongation at rupture. The data were analyzed according to the classical phenomenological / physical relations (Norton, Arrhenius, Zenner-Hollomon, Monkman-Grant) and also considering five traditional parameterization methodologies (Larson-Miller, Orr-Sherby-Dorn, Goldhoff-Sherby, Manson- Haferd and Manson-Succop). Comparisons are presented among the possibilities of data extrapolation from five different methodologies. Comparison is also made with creep results obtained on a similar plate of the same material in the virgin condition.

Keywords: 1Cr0.5Mo steel - Ex-service Condition; Constant stress creep; Creep relations; Data Parameterization.

[1] *PhD/Materials Engineering, Associate Professor / Retired from Materials.Engineering Dept. / UFSCar, São Carlos-SP. Now at STM-Systems for Testing of Materials Ltda., São Carlos-SP, Brazil.*

ISSN 1516-392X

1 INTRODUCTION

During a scheduled shutdown, for maintenance, a section of a heavy wall plate was extracted from a FCC (Fluid Catalytic Cracking) Reactor of a petrochemical plant. The plate was manufactured with 1Cr0.5Mo steel and operated for about 17 years (~ 150.000 h) at a nominal temperature of 565ºC and one of the main concerns was the determination of its creep properties within a work program for its residual life assessment.
The characterization of the creep behavior of the material was performed using constant stress creep machines having high sensitivity instrumentation in a British creep laboratory.
Another section of similar plate of the same material in the virgin condition was also considered for comparison and it was tested in the same laboratory. Due to the large amount of data generated in this project, however, in the present work (Part 2), only the analysis of the results on the ex-service material will be presented. In another article in this conference (Part 1) [1] the analysis of the results on the virgin material is also included. The present work also describes a comparison between the results on both materials.
The main objective in this article is the description of the results according to the traditional procedures of creep behavior and data extrapolation analysis, proposed by various authors.
As mentioned in Part 1 of this work [1], another important objective of the work was the analysis of all these data according to the Theta-Projection methodology proposed by Evans and Wilshire [2-4]. However, due to the large amount of information on this subject, the results of that work will be presented in a future publication.

2. MATERIALS AND METHODS

The material consisted in the 1Cr0.5Mo steel type A387 Grade 12 CL2 which is largely employed in high temperature systems.
Figures 1a and 1b show the microstructure of the material in the ex-service condition and Figures 1c and 1d the microstructure in the virgin condition, for comparison. The material had originally a structure of grains of about 80% pro-eutectoid ferrite and 20% tempered bainite. After service, the structure reveals considerable changes with the grains of bainite suffering intensive dissolution and coarsening of carbides, and the ferrite grains showing massive inter and intra-granular precipitation.
Creep specimens with cylindrical shape were obtained from the ex-service sample, having shoulders with thread M12x1.75 and gauge-length Lo = 25mm and diameter Do = 6.25mm.Creep tests were carried out in *constant stress* type Dennison machines having load-levers equipped with Andrade-Chalmers profiles (cams). The furnaces operated with micro-processed temperature controllers capable of maintaining the temperature within ± 1ºC during the tests. High temperature extensometers employing SLVC transducers were used to monitor the elongation of the specimens. The readings of elongation and time were collected by an ASL Data Logger system that could be programmed to make scanning in the whole group of creep machines at appropriate time intervals. Twenty three specimens of the ex-service material were tested using a set of 10 creep machines, that operated during about 12000 h.

ISSN 1516-392X

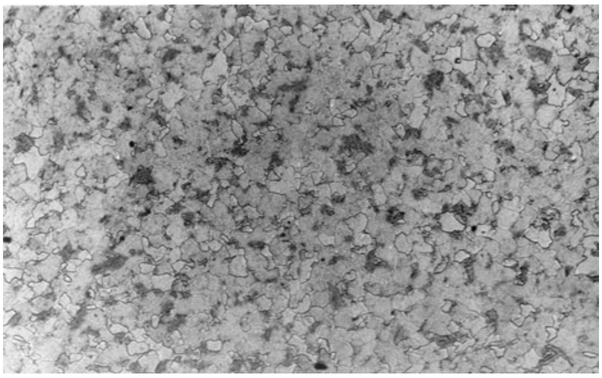

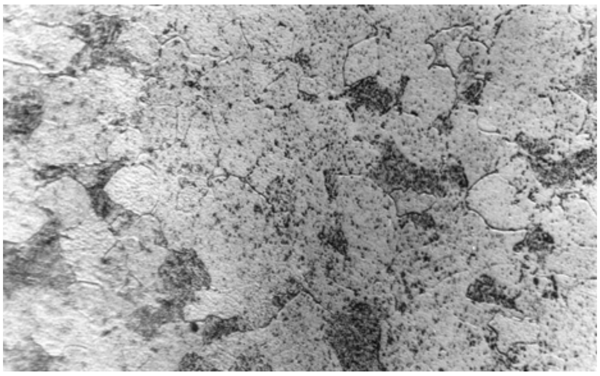

a) [original magnification100x] b) [original magnification 400x]

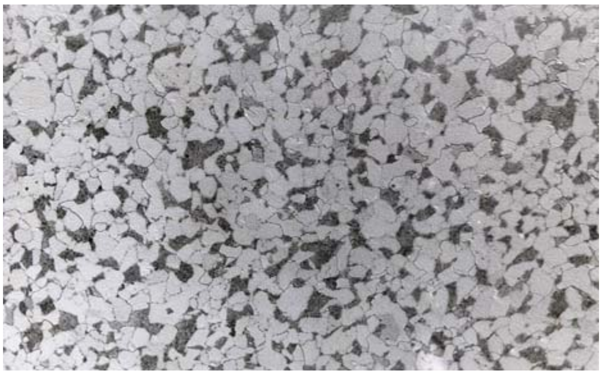

c) [original magnification100x] d) [original magnification 400x]

Figure 1 – Optical micrographs of the material: a) and b) in the Ex-Service condition, after 17 years of service in the FCC reactor, at a nominal temperature of 565ºC; c) and d) in the Virgin condition.

Three levels of temperature were selected for this research: 811K (538ºC), 838K (565ºC) and 866K (593ºC). The applied stresses varied in the range from: 52 to 224 MPa, producing rupture times lasting from about 5 to 4000 h.
The creep curves were all followed with great scrutiny using data logger scanning rates which enabled storing thousands of readings in each case. This was necessary for the analysis of the data according to the Theta-Projection methodology, which will be the subject of a future publication.
The analysis of the data relative to the present article (Part 2) involved determination of the variation of minimum creep rate, the rupture time, the final elongation of the specimens in terms of temperature and stress used in the tests.

3 RESULTS AND DISCUSSION

Figure 2a shows a plot of LOG(Stress) versus LOG(Rupture Time) , i.e. the Loss of Creep Rupture Strength with Time exhibited by the material at the three temperatures investigated.
Figure 2b shows the creep data plotted in the form of a Norton diagram, i.e. LOG(Stress) versus LOG(Rupture Time), used to verify the validity of the Norton relation: $\dot{\varepsilon}_s = A'\sigma^n$ at a certain iso-temperature condition ($\dot{\varepsilon}_s$ = Secondary or Minimum Creep Rate, σ = Applied Stress, with A' and n constants). Straight lines fitted to each set iso-temperature data gives n=7.2 for 866K, n=8.3 for 838K and n=8.8 for 811K.
Figure 3a shows the creep data plotted in the form of an Arrhenius diagram, i.e. LN(Minimum Creep Rate) versus 1/T, used to verify the validity of the relation: $\dot{\varepsilon}_s = A''\exp(-Q_c/RT)$ at a certain iso-stress condition ($\dot{\varepsilon}_s$=Secondary or Minimum Creep

ISSN 1516-392X

Rate, T= temperature, with A'' and Q_c (Apparent Creep Activation Energy) constants).

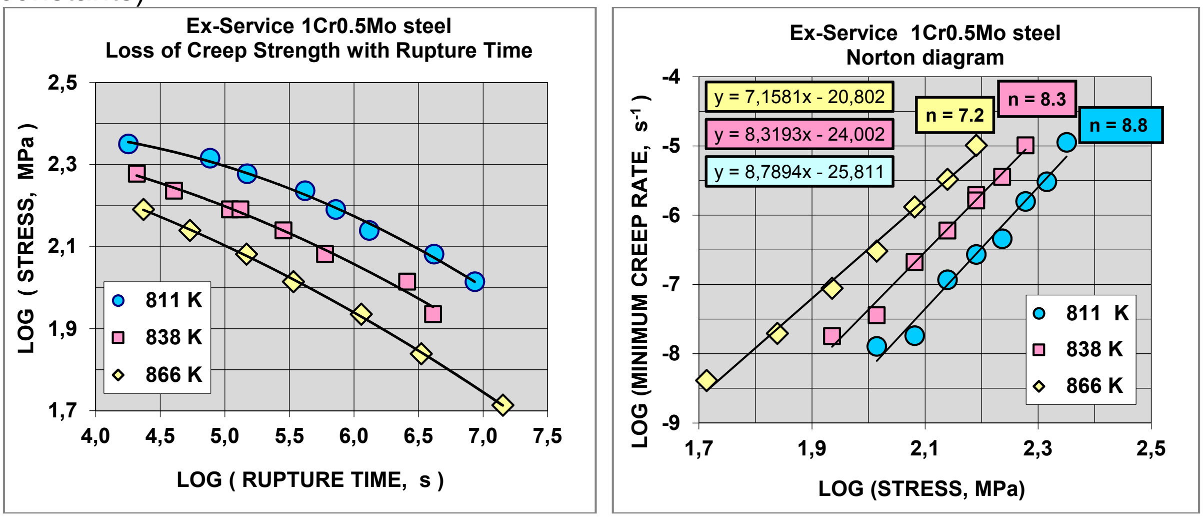

a) b)

Figure 2 - a) Loss of Creep Rupture Strength with Time; b) Norton diagram.

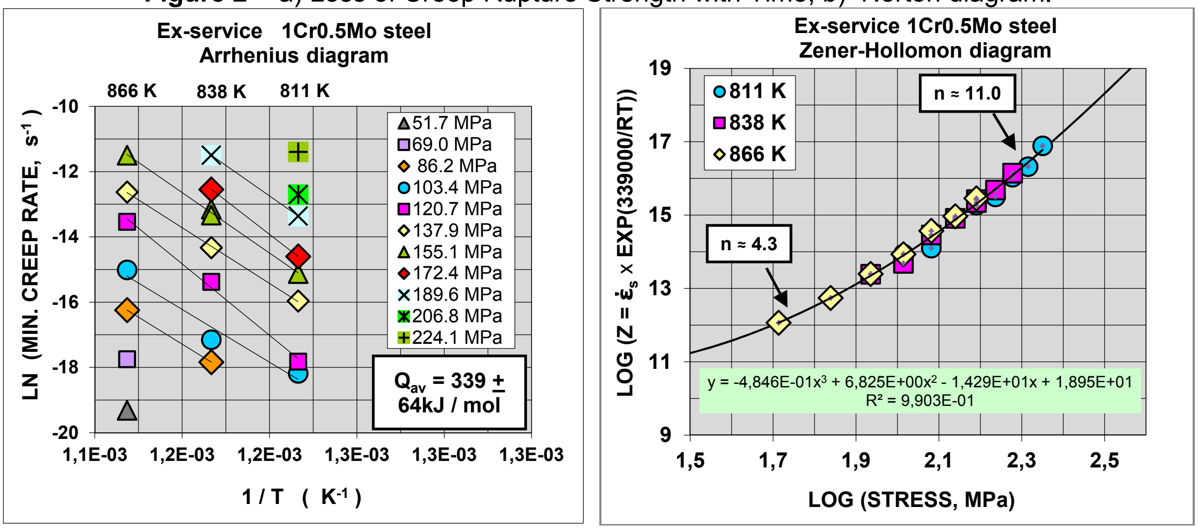

a) b)

Figure 3 - a) Arrhenius diagram, b) analysis of the data using the Zener-Hollomon parameter.

Straight lines fitted to each iso-stress set of data produces an average value for the apparent creep activation energy of Q_c = 339 kJ/mol.

The data shown in Figure 2b in the form of a Norton diagram can be rationalized using the Zener-Hollomon parameter, defined as: $Z = \dot{\varepsilon}_S \,.\, \exp(-Q_c/RT)$, taking Q_c = 389 kJ/mol. As shown in Figure 3b, when LOG(Z) is plotted in terms of LOG(σ), the three iso-temperature sets of data of Figure 2b collapse in the form of a single reference curve, so that creep behavior is better expressed by: $Z = A''' \sigma^n$. It can be observed that this reference curve is not a straight line, i.e. the value of n is not constant, as the stress varies. In fact, in the lower range of stress the value of n is about $n \approx 4.3$ whilst in the higher range $n \approx 11$. A 3rd degree polynomial was well fitted to the data, although it not at all reliable to be used for extrapolation of the data much beyond the experimental data range.

Figure 4a shows the creep data plotted in the form of the Monkman-Grant diagram, so as to verify the validity of the Monkman-Grant relation: $\dot{\varepsilon}_S \,.\, t_r^m = K$ (t_r = rupture time, m and K constants). The present data showed the value of m =1.1872 and

ISSN 1516-392X

K =1.578. The Monkman-Grant plot makes a kind of natural parameterization of the data of LOG($\dot{\varepsilon}_s$) in terms of LOG(t_r). However, it is well known that these kinds of plots show always a considerable degree of scatter [2]. In this article we suggest the possibility of rationalization of the Monkman-Grant plot using the Zener-Hollomon parameter, instead of Minimum Creep Rate in the Y-axis, and the Temperature Compensated Rupture Time, instead of Rupture Time in the X-axis, i.e. $\Theta = t_r.\exp(-Qc/RT)$. When this is done, the new plot shows less scatter, as can be observed in Figure 4b. The new Monkman-Grant relation could be expressed now by:

$$Z \,.\, \Theta^{m'} = K^* \qquad \text{with } m' \text{ and } K^* \qquad (1)$$

with parameterization of the data in the X and Y axis.

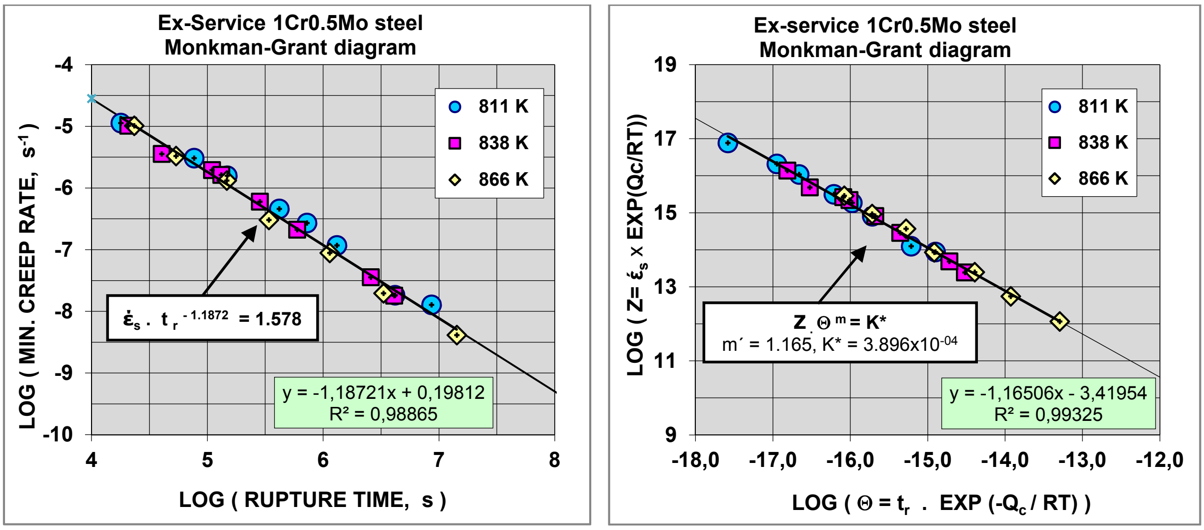

a) b)

Figure 4 – a) Monkman-Grant diagram; b) rationalization of the Monkman-Grant diagram using the Z and Θ parameters.

Figure 5a shows the creep data plotted in the space LOG(t_r) versus 1/T. This is the kind of graph that must be organized to inspect the possibility of parameterization according to the methods of Larson-Miller, Orr-Sherby-Dorn and Goldhoff-Sherby [5]. Figure 5b shows the same data plotted in the space LOG(t_r) versus T, which is used for exploring the possibility of parameterization by the methods of Manson-Haferd and Manson-Succop. In both cases, the least-square procedure of Manson-Mendelsohn [6] was used to derive the values of the constants of each method.
The parameters of these methods are defined by the following relations:

Larson-Miller Parameter: $LMP = T[C + LOG(t_r)]$ (1)

Orr-Sherby-Dorn Parameter: $OSDP = LOG(t_r) – A/T$ (2)

Goldhoff-Sherby Parameter: $GSP = – [LOG(t_r) – LOG(t_r)^*] / [1/ T – (1/T)^*]$ (3)

Manson-Haferd Parameter: $MHP = – (T – T^*)/[LOGt_r - LOG(t_r)^*]$ (4)

Manson-Succop Parameter: $MSP = LOG(t_r) – BT$ (5)

where C, A, LOG(tr)*, (1/T)*, T* and B are constants determined by the Manson-Mendelsohn procedure [6].

ISSN 1516-392X

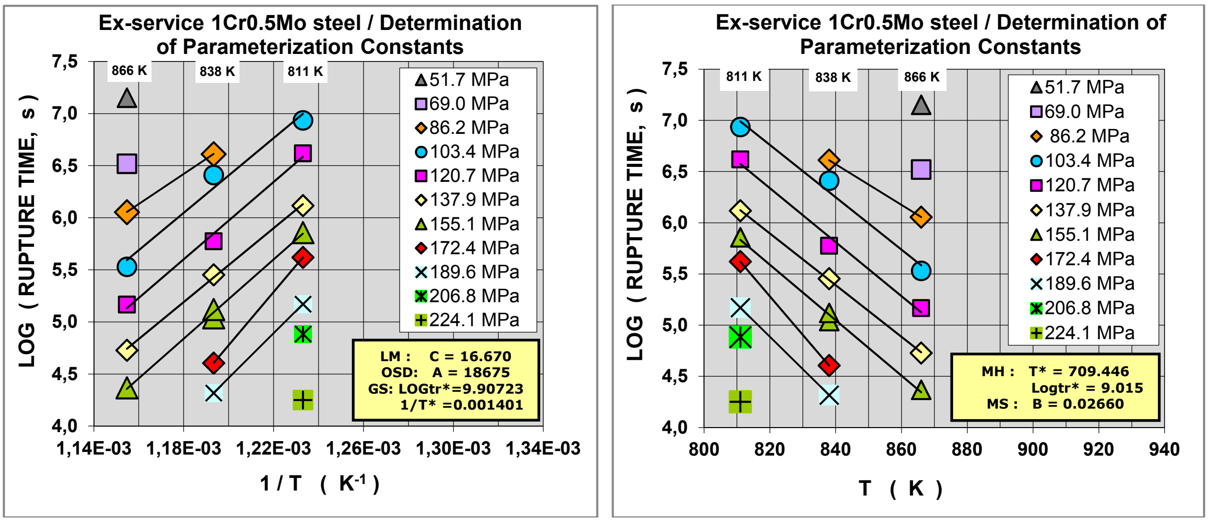

a) b)

Figure 5 - Plot of LOG(tr) versus 1/ T to verify possibility of parameterization by the methods of Larson-Miller, Orr-Sherby-Dorn and Goldhoff-Sherby ; plot of LOG(tr) versus T to verify possibility of parameterization by the methods of Manson-Haferd and Manson-Succop.

Figure 6 presents the 5 parameterization curves obtained with this analysis. The constants involved in each method are specified in each figure. In each case, low degree polynomials (2nd degree) are usually fitted to the data. The quality of fit of each methodology can be judged from the values of the corresponding correlation coefficients R^2. The best fit was achieved with the Orr-Sherby-Dorn analysis (R^2 = 0.99520). In the sequence comes the analysis with: Manson-Succop (R^2 = 0.99476), Larson-Miller (R^2 = 0.99421), Manson-Haferd (R^2 = 0.99283) and Goldhoff-Sherby (R^2 = 0.99206) methodologies. The Manson-Haferd analysis produced an unrealistic curve with different shape in relation to the virgin material [1]. It seems that more data would be necessary for a better definition of the Manson-Haferd constants in this case. Therefore, the parameterization curve of the Orr-Sherby-Dorn methodology was selected for extrapolation of the data of the ex-service material. The constant A determined by the Manson-Mendelsohn analysis in this methodology was A = 18675.
The predictive quality of the Zener-Hollomon analysis in predicting the minimum creep rate data is shown in Figure 7a. In the same way, the predictive quality of the Orr-Sherby-Dorn analysis in predicting the rupture time data is shown in Figure 7b. It can be noticed that in both cases the agreement of the iso-temperature lines at 811K, 838K and 866K with the corresponding experimental points is excellent. The better performance of the Orr-Sherby-Dorn analysis in the present results also agrees with the parametrization of the Monkman-Grant data (Figure 4a) in terms of Z as function of the Temperature Compensated Rupture Time:

$$\Theta = t_r \, . \, \exp(-Qc/RT) \qquad 6$$

as proposed in this article. The Θ parameter is closely related to the OSDP, since:

$$LOG(\Theta) = LOG(tr) - LOG(e).(Qc/RT)$$

and therefore:

$$LOG(\Theta) = OSDP \qquad 7a$$

and

$$A = Qc.LOG(e)/R \qquad 7b$$

Since A=18675 for the ex-service material → Qc = 357 kJ/mol, a value that is rather close to Qc=339 kJ/mol determined from the Arrhenius diagram in Figure 3a.

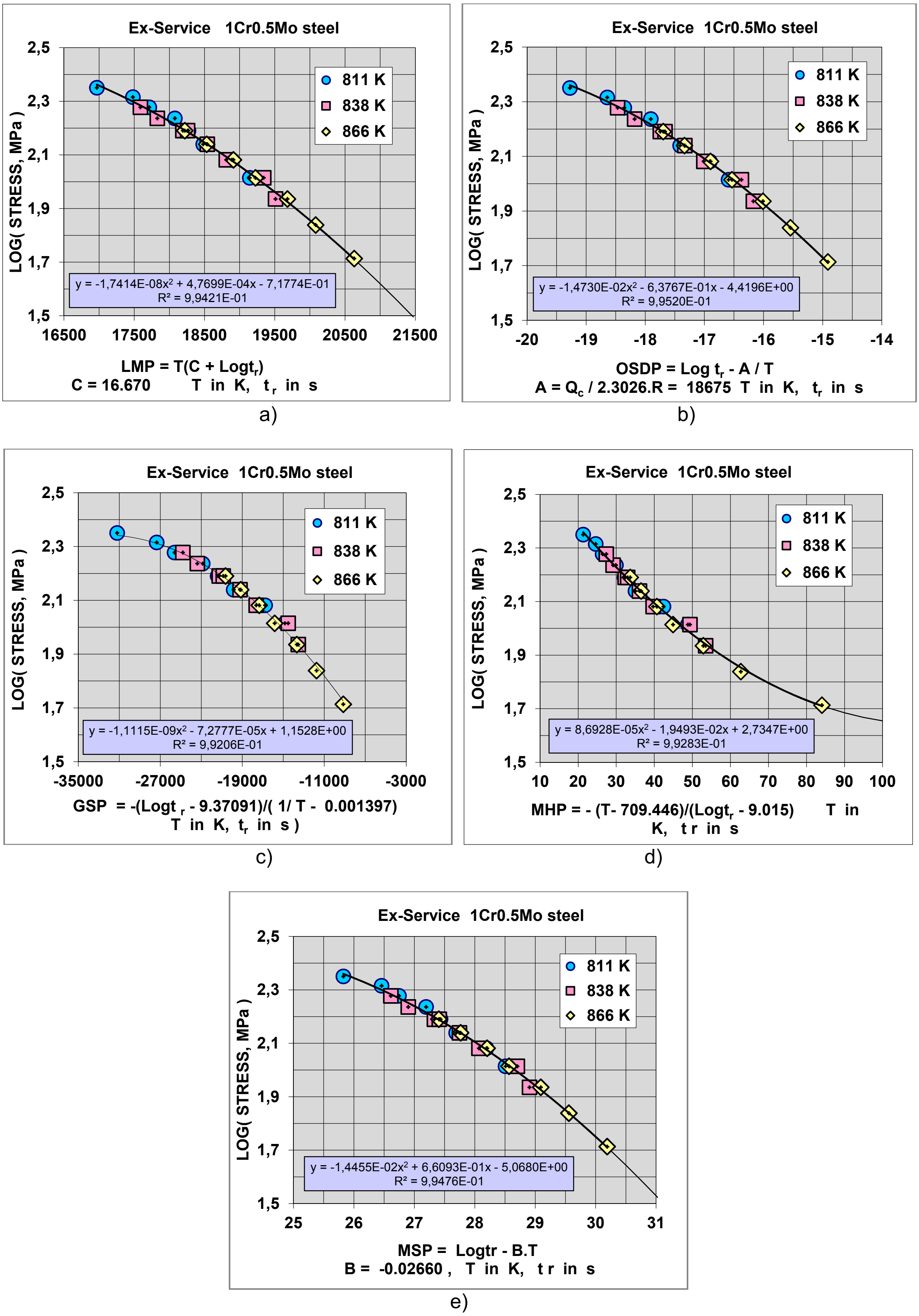

Figure 6 - Parameterization by the methods of: a) Larson-Miller; b) Orr-Sherby-Dorn; c) Goldhoff-Sherby; d) Manson-Haferd; e) Manson-Succop.

ISSN 1516-392X

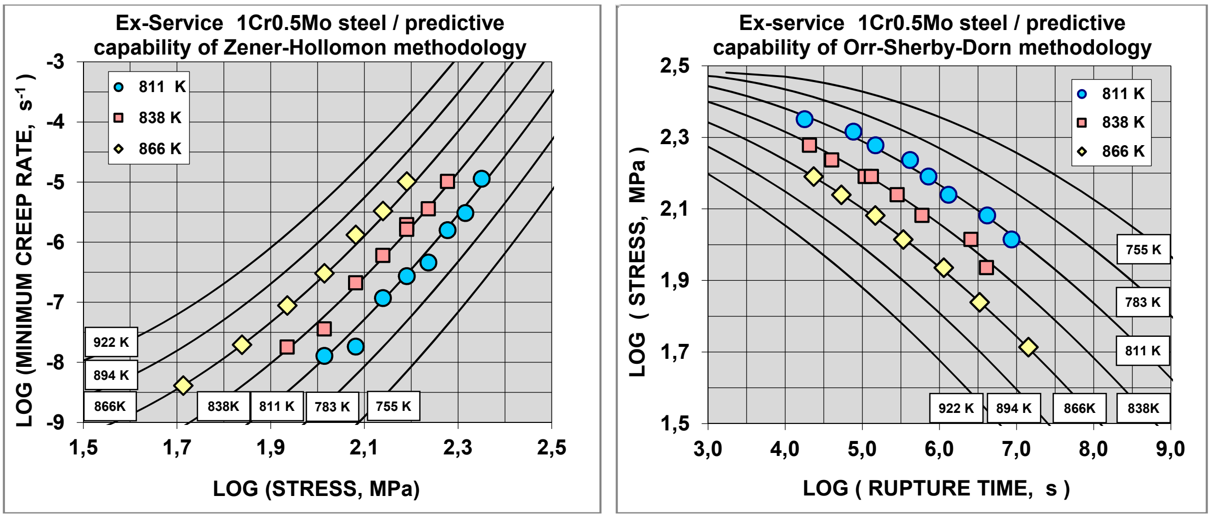

Figure 7 – Predictive Capability of the: a) Zener-Hollomon parameterization; b) Orr-Sherby-Dorn parameterization.

As mentioned in the Introduction of this article, a similar plate of the same steel, but in the virgin condition, was also studied in similar creep test conditions to enable a comparison with the ex-service material results.

Figure 8a shows the Zener-Hollomon parameterization curves for the two materials. The curve of the ex-service material is situated above the curve of the virgin material, as expected. In the lower stress range (below stresses used in this work) both materials seem to show coincidence with each other.

For the virgin material it was observed that the best parameterization curve was also obtained with the Orr-Sherby-Dorn methodology, but with A = 20271. To enable comparison between the two parameterization curves, a value of an average constant A = 19473 was used in both situations.

Figure 8b shows the OSD curves of the virgin and the ex-service materials. It is evident that the ex-service material presents a considerable drop in creep strength in relation to the virgin material.

In the high stress level, for a value of POSD = -19, for instance, a drop from 267MPa (in the virgin condition) to 196MPa (in the ex-service condition) would happen at 565ºC in short creep rupture times of about 5 h. In the lower stress level, for a value of POSD = -15.2, for instance, a drop from 58MPa (in the virgin condition) to 48MPa (in the ex-service condition) would happen at 565ºC in creep rupture times of about 3.5 years. The determination of the relative position of the ex-service and the virgin curves is certainly o great importance in residual life estimations of the material.

Figure 8c presents a comparison between the Monkman-Grant data of the virgin and the ex-service material. The straight line of the ex-service material is situated below the straight line of the virgin material, with a trend for coincidence at low rupture times, but diverging progressively downwards for higher rupture times. This is a reflection of the higher value of m of the ex-service material (1.1872) in relation to the virgin material (1.0356), which implies loss of creep ductility of the material when exposed to service conditions [7].

Figure 8d shows the same kind of comparison in relation to the parameterized Monkman-Grant data of both materials. The same features commented in relation fo Figure 8c are basically observed.

Figure 9a depicts the variation in creep ductility (represented by the final percentage elongation measured in each test) with stress at the three investigated temperatures.

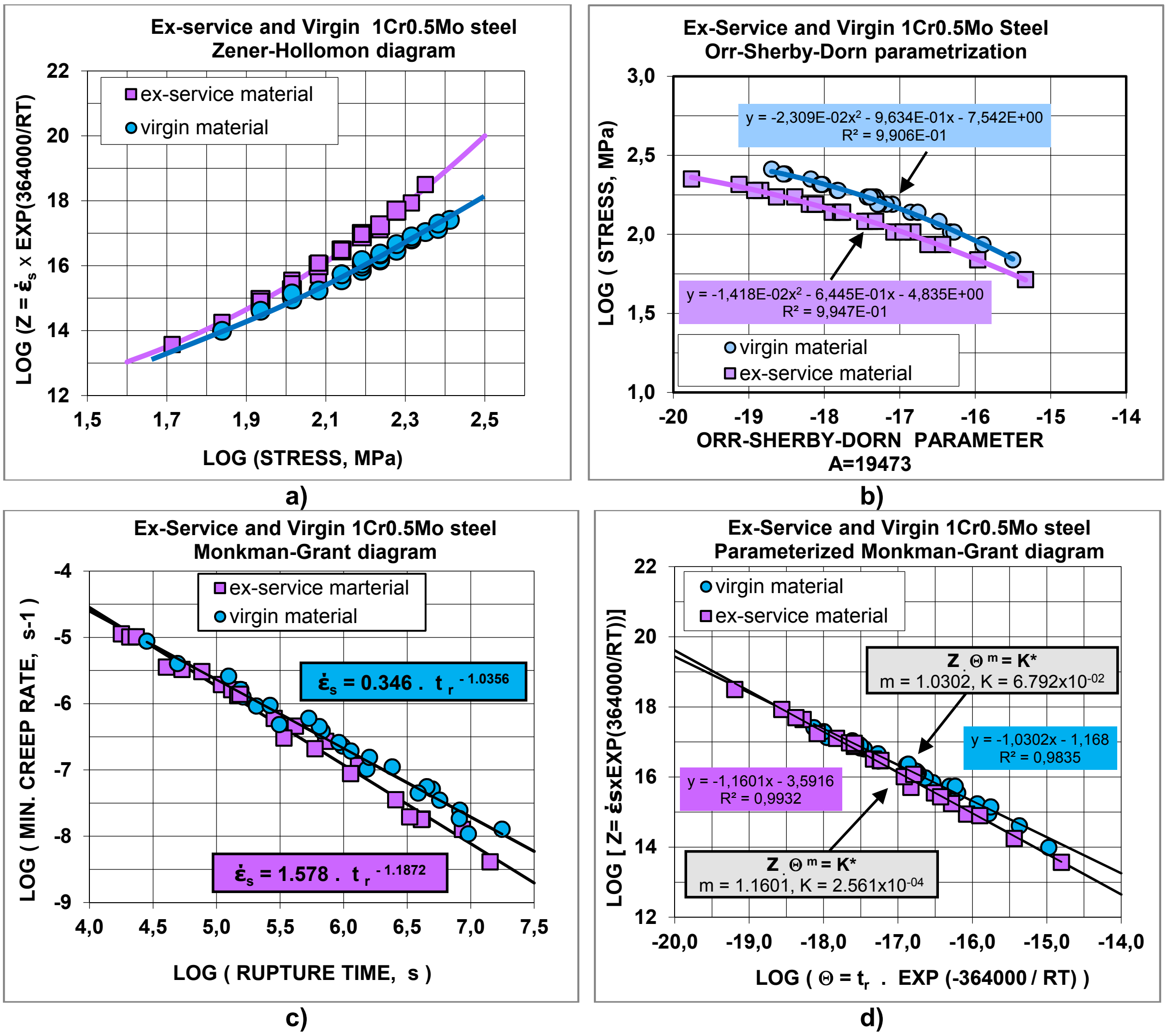

Figure 8 – Comparison of the Virgin and Ex-Service parameterization curves obtained with: a) The Zener-Hollomon parameter; b) the Orr-Sherby-Dorn methodology; c) the Monkman-Grant diagram; d) the parameterized Monkman-Grant diagram.

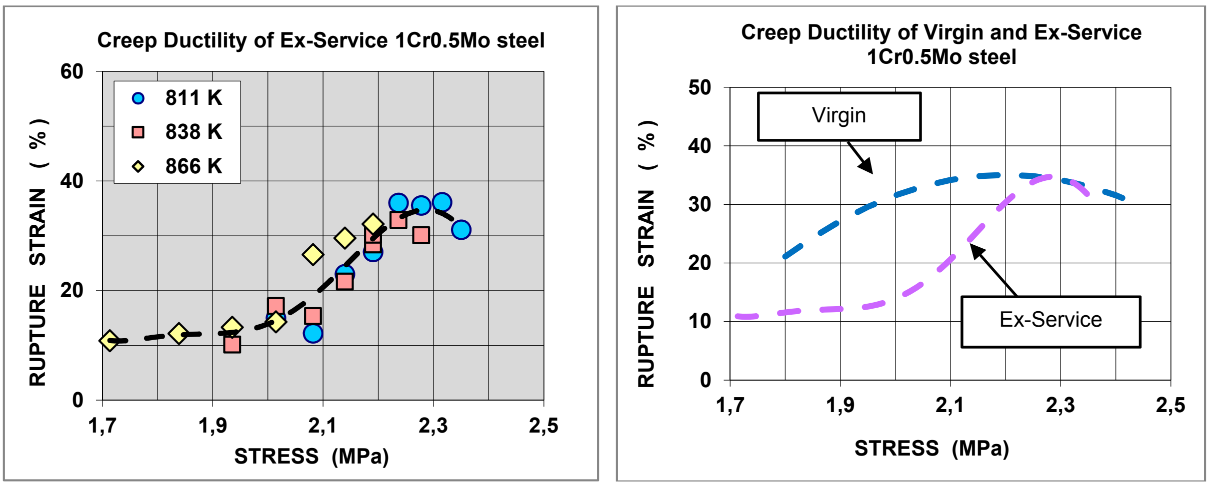

Figure 9 – Creep ductility of 1Cr0.5Mo steel: a) in the ex-service condition; b) comparison between the virgin and ex-service conditions.

In the stress range from about 50 to 100 MPa the creep ductility remains constant at a level of 10%. For stress greater than 100 MPa there is an increase up to about 35% that seems to be a peak at about 170 MPa with a drop thereafter.

Figure 9b brings a comparison with data of creep ductility obtained from the virgin material. In this case the creep ductility is much higher than in the ex-service condition, increasing monotonically from 20% up to a maximum of about 35% at 140 MPa and decreasing to about 30% at 250 MPa. It seems that the creep ductility was depleted during service due, specially, to the extensive precipitation and coalescence of inter and intra-granular carbides, as shown in Figures 1c and 1d, compared to Figures 1a and 1b.
The use of the extrapolation curve in Figure 6b is reliable only for prediction up to about 40,000 h, i.e. maximum of one LOG cycle beyond the experimental range attained in this work. The extrapolation can also be made more reliable if instead of a 2nd degree polynomial a more appropriate function is used to fit the data in Figure 6b, such as the Spera function, for instance [8].
With the Theta-Projection analysis, however, according to the authors [2], extrapolation is reliable up to 100,000 h or even more with the present results. The creep data obtained in this work with the virgin and ex-service materials were also analyzed according to this methodology, but the results will be the subject of another publication.

4 CONCLUSION

The characterization of creep behavior of a heavy-wall plate of ex-service 1Cr0.5Mo steel extracted from a FCC Reactor subjected to operation for about 17 years at a nominal temperature of 565^{o}C produced the following results, for constant stress tests in the range from 52 to 224 MPa, at three temperature levels (811, 838 and 866K):

a) Norton diagram produced the following n values for the material: n= 7.2, 8.3 and 8.8 for: T= 866K, 838K and 811K, respectively.
b) Arrhenius diagram indicated an average Apparent Creep Activation Energy Qc=339 $\pm$ 64 kJ/mol for the material.
c) Zener-Hollomon parameterization, with Qc=339 kJ/mol, was effective in transform Norton diagram in a single reference curve, with the stress exponent varying from n=4.3 to n=11.0, at the lower and higher stress levels, respectively.
d) Monkman-Grant diagram produced values of m=1.1872 and K=1.578 in the relation: $\dot{\varepsilon}_s \, . \, t_r^m = K$, with $\dot{\varepsilon}_s$ in s^{-1} and t_r in s.
e) Monkman-Grant diagram can be parameterized using the Zener-Hollomon parameter and the temperature compensated rupture time: $\Theta = t_r.\exp(-Qc/RT)$, so that the relation: $Z \, . \, \Theta^{m'} = K^*$ is valid with m´= 1.165 and K* = 3.896×10^{-04}.
f) Five methods from the traditional parameterization literature were tested with the present results and the best result was obtained with the Orr-Sherby-Dorn analysis, with a constant A = 18675.
g) Comparison between the Orr-Sherby-Dorn curves of the ex-service material and the virgin material reveals a considerable loss of creep strength due the microstructural degradation of 1Cr0.5Mo steel during service. At 565^{o}C creep strength varied from 267 MPa to 196 MPa for short time tests of about 5 h duration, and from 58MPa to 48 MPa for long time tests of about 3.5 years duration, for the virgin the ex-service material, respectively.
h) The lower creep strength of the ex-service material is also confirmed by its higher n values and lower Qc value in relation to the virgin material.

i) Creep ductility has also been significantly reduced specially in the low and intermediate stress range investigated. The reduction in creep ductility of the ex-service material is also revealed by their Zener-Hollomon and Monkman-Grant plots when compared to the virgin material.

Acknowledgments

The author acknowledges The Federal University of São Carlos and the Department of Materials Engineering for conceding a license of study in the UK and the provision of a grant by FAPESP-Fundação de Amparo à Pesquisa do Estado de São Paulo to support his stage at the Engineering Materials Department / Swansea University in Wales during two years. Acknowledgements are also due to Prof. Brian Wilshire for his permission to use 10 constant stress creep machines in this project at IRC-Interdisciplinary Research Center/USW and also to Dr. Miles Davis for his technical assistance during the experimental work in the Creep Laboratory. Special thanks are also due to José Cláudio GuimarãesTeixeira from CENPES-Petrobrás, Rio de Janeiro (RJ), for supplying the samples of the materials used in this research.

REFERENCES

1 Bueno LO. Creep Behavior of Virgin 1Cr0.5Mo Steel. Part 1 – Analysis based on the Theta Methodology approach. Proc. ABM Week 2015 – 70th ABM Annual Congress,17–20 August, Rio de Janeiro(RJ), Brazil.

2 Evans RW, Wilshire B. Creep of Metals and Alloys. The Institute of Metals. London, UK, 1985.

3 Wilshire B, Scharning PJ. A new methodology for analysis of creep and creep fracture data for 9–12% chromium steels. Inter Mater Ver. 2008. 53: 91-104.

4 Harrison W, Whittaker M, Williams S. Recent Advances in Creep Modelling of the Nickel Base Superalloy – Alloy 720Li. Materials. 2013. 6: 1118-1137.

5 Visvanathan R. Damage Mechanisms and Life Assessment of High-Temperature Components, ASM International, Palo Alto, CA, USA, 1993.

6 Penny RK, Mariott DL. Design for Creep. Chapman and Hall, 2nd Edition, Padstow-UK, 1995.

7 Phaniraj C, Choudhary BK, Rao KBS, Raj B. Relationship between time to reach Monkman–Grant ductility and rupture life. 2003**.** Scripta Materialia**,** 48/9: 1313-1318.

8 Furtado HC, Almeida LH, LeMay I. Damage and remaining life estimation in high temperature plant with variable operating condition. Ohmni. 2008. 5: 1-1.Issue 1-May 2008-www.ohmni.co.uk.